Fish & Shellfish Immunology 46 (2015) 624–637

Contents lists available at ScienceDirect

Fish & Shellfish Immunology

journal homepage: www.elsevier.com/locate/fsi

Full length article

Impact of feed additives on surface mucosal health and columnaris susceptibility in channel catfish fingerlings, *Ictalurus punctatus*

Honggang Zhao [a], Chao Li [b], Benjamin H. Beck [c], Ran Zhang [a], Wilawan Thongda [a], D. Allen Davis [a], Eric Peatman [a, *]

[a] School of Fisheries, Aquaculture, and Aquatic Sciences, Auburn University, Auburn, AL 36849, USA
[b] Marine Science and Engineering College, Qingdao Agricultural University, Qingdao 266109, China
[c] United States Department of Agriculture, Agricultural Research Service, Stuttgart National Aquaculture Research Center, Stuttgart, AR 72160, USA

ARTICLE INFO

Article history:
Received 1 May 2015
Received in revised form
26 June 2015
Accepted 6 July 2015
Available online 9 July 2015

Keywords:
Siluriformes
Flavobacterium columnare
RNA-seq
Mannan oligosaccharides
Prebiotic
Nutri-genomics

ABSTRACT

One of the highest priority areas for improvement in aquaculture is the development of dietary additives and formulations which provide for complete mucosal health and protection of fish raised in intensive systems. Far greater attention has been paid to dietary impact on gut health than to protective effects at other mucosal surfaces such as skin and gill. These exterior surfaces, however, are important primary targets for pathogen attachment and invasion. *Flavobacterium columnare*, the causative agent of columnaris disease, is among the most prevalent of all freshwater disease-causing bacteria, impacting global aquaculture of catfish, salmonids, baitfish and aquaria-trade species among others. This study evaluated whether the feeding of a standard catfish diet supplemented with Alltech dietary additives Actigen®, a concentrated source of yeast cell wall-derived material and/or Allzyme® SSF, a fermented strain of Aspergillus niger, could offer protection against *F. columnare* mortality.

A nine-week feeding trial of channel catfish fingerlings with basal diet (B), B + Allzyme® SSF, B + Actigen® and B + Actigen®+Allzyme® SSF revealed good growth in all conditions (FCR < 1.0), but no statistical differences in growth between the treatments were found. At nine weeks, based on pre-challenge trial results, basal, B + Actigen®, and B + Allzyme® SSF groups of fish were selected for further challenges with *F. columnare*. Replicated challenge with a virulent *F. columnare* strain, revealed significantly longer median days to death in B + Allzyme® SSF and B + Actigen® when compared with the basal diet ($P < 0.05$) and significantly higher survival following the eight day challenge period in B + Actigen® when compared with the other two diets ($P < 0.05$). Given the superior protection provided by the B + Actigen® diet, we carried out transcriptomic comparison of gene expression of fish fed that diet and the basal diet before and after columnaris challenge using high-throughput RNA-seq. Pathway and enrichment analyses revealed changes in mannose receptor DEC205 and IL4 signaling at 0 h (prior to challenge) which likely explain a dramatic divergence in expression profiles between the two diets soon after pathogen challenge (8 h). Dietary mannose priming resulted in reduced expression of inflammatory cytokines, shifting response patterns instead to favor resolution and repair. Our results indicate that prebiotic dietary additives may provide protection extending beyond the gut to surface mucosa.

1. Introduction

Fish currently provides three billion people with 20% of their animal protein requirements. However, environmental pollution and overexploitation threaten natural fish stock regeneration [1,2]. To meet the increased demand from the global market, aquaculture will play an increasingly important role in contributing to the volume and stability of global fish supplies. Commercial fish farming, in tanks or enclosures under monitored conditions, can increase production by controlling variables ranging from exclusion of predators and improved water quality to enhancement of diet and nutrition [3]. However, intensive aquaculture has been traditionally accompanied by increasing incidence and severity of disease outbreaks as environmental, genetic, or nutritional deficiencies are exploited by primary and opportunistic pathogens.

* Corresponding author.
E-mail address: peatmer@auburn.edu (E. Peatman).

http://dx.doi.org/10.1016/j.fsi.2015.07.005
1050-4648/

Developing dietary supplements and additives to provide complete mucosal health and protection of fish raised in intensive systems has emerged, therefore, as a high priority area with a great potential for significant improvements in aquaculture.

Teleost fish exhibit well-developed physical and immunological barriers at mucosal surfaces where a complex interplay of secreted mucus, commensal bacteria, and underlying mucosa-associated lymphoid tissue (MALT) elements serve to co-regulate immunity and maintain homeostasis in healthy fish [4,5]. While our understanding of host-pathogen-commensal-environment interactions are growing, our knowledge has been, until recently, focused in the gut mucosa, with relatively little study on skin and gill barriers. These exterior surfaces, however, are important primary targets for pathogen attachment and invasion. A key question is whether dietary additives, known to enhance gut immune health [6,7], may also stimulate beneficial, protective immunity at distal mucosal surfaces, either through transfer through the blood or by direct stimulation of immune receptors through the presence of whole or digested feed components in the water [8].

Flavobacterium columnare, the causative agent of columnaris disease, is among the most prevalent of all freshwater disease-causing bacteria. Often characterized as unpredictable and difficult to treat, columnaris impacts global aquaculture of catfish, salmonids, baitfish and aquaria-trade species among others [9,10]. Channel catfish, the predominant aquaculture species in the United States, are exceedingly susceptible to columnaris disease [11]. Catfish experiencing stress due to high rearing density [12], high organic loads [13], excessive handling [14], or high ammonia etc. [15] are more susceptible to *F. columnare* infection. Catfish gill and skin tissues constitute the primary route of entry for the pathogen, with infection often grossly evident soon after colonization in the form of pale discoloration, erosion or necrosis of these tissues [16]. Strategies to combat columnaris infections have long included lowering rearing density, salt baths, acid baths, and chemical therapeutants [17]. However, these approaches have failed to reduce columnaris disease incidence, as they are largely reactive measures after the onset of disease. Cost-effective, improved dietary formulations which improve immune readiness or decrease pathogen adhesion offer the potential of continuous, proactive mucosal protection [18,19].

High-throughput transcriptome sequencing (RNA-seq) offers several advantages over traditional microarray approaches for nutri-genomics [20]. It allows for capture of novel transcripts and splicing variants which may not be present on static arrays, it has a larger dynamic range, and it avoids the potential of cross-hybridization of similar probes resulting in inaccurate gene expression values [21]. Using RNA-seq approaches, previous work by our group has demonstrated that differing cytokine and lectin profiles in surface mucosa differentiate fish from families identified as resistant or susceptible to columnaris disease [4]. We have particularly focused on the role of a rhamnose-binding lectin (RBL1a) in facilitating pathogen attachment and invasion in the gill [4,22–24]. Our group found that pathogen attachment could be reduced in a dose-dependent manner through addition of a sugar ligand (rhamnose or D-galactose) and that levels of RBL1a were dramatically impacted by feeding status [22]. Given our improved understanding of mechanisms potentially governing host mucosal immunity in the context of columnaris, we were interested in examining whether commercially-available enhanced diets could increase catfish survival by modulating these same pathways. It was investigated whether the feeding of a standard catfish diet supplemented with Alltech dietary additives Actigen®, a concentrated source of yeast cell wall-derived material including mannan oligosaccharides (MOS) and/or Allzyme® SSF, a fermented strain of *Aspergillus niger* producing a complex of enzymes [25], could offer protection against *F. columnare* mortality.

2. Material and methods

2.1. Fish and diet composition

All procedures involving the handling and treatment of fish used during this study were approved by the Auburn University Institutional Animal Care and Use Committee (AU-IACUC) prior to initiation.

In order to evaluate the biological response of two dietary supplements (Actigen® and Allzyme® SSF meals, Alltech, Inc., Nicholasville, KY, USA), four practical diets (Basal diet (B), B + Allzyme® SSF, B + Actigen® and B + Actigen®+Allzyme® SSF) were formulated to contain 36% protein and 8% lipids and offered to juvenile (average size 4.1 ± 0.11 g) channel catfish over a nine week growth trial (Table 1). Fish were stocked in 36 aquaria (75L) at a density of 20 fish per aquaria with nine replicate tanks per dietary treatment. The fish in the replicate aquaria were randomly assigned to each dietary treatment and offered feed twice daily (8:00 am, 4:00 pm) based on a set percentage of body weight. Water temperature (27.82 ± 1.16 °C) and dissolved oxygen (5.63 ± 0.73 mg/L) were measured twice daily by YSI Model 58 Oxygen Meter (Yellow Springs Instrument Model 58, Yellow Springs, OH, USA) and pH (7.23 ± 0.40) weekly with a pH meter. A diel light:dark cycle was set at 14:10 h. Fish were weighed upon initiation of the trial and every two weeks thereafter. Feed inputs were adjusted based on observed feed consumption and biweekly feed conversion ratio. At the conclusion of the growth trial, final weight, weight gain and feed utilization were determined. All data was analyzed using one-way analysis of variance to determine significant differences ($P < 0.05$) among treatments. The statistical analyses were performed using the SAS® software package (SAS Institute Inc., Cary, NC, USA).

The basal diet was formulated to meet the known nutrient requirements of the fish and represents a typical fingerling diet. Diets were manufactured at Auburn Fisheries North Station, Auburn, AL under laboratory conditions. Each diet was prepared by mixing pre-ground dry and wet ingredients in a food mixer (Hobart, Troy, OH, USA) for 15 min. Boiling water was then blended into the mixture to attain a consistency appropriate for pelleting. The moist mash from each diet was passed through a die (2.4 or 3.17 mm) in a meat grinder, and the pellets were dried in a forced air drying oven (<50 °C) to a moisture content of less than 10%. Diets were stored at −20 °C and prior to use each diet was ground and sieved to an appropriate size.

2.2. Bacterial challenge and tissue collection

Fish were maintained in four 50 gallon tanks and acclimatized for 2 weeks at a temperature of 28 °C after transfer to the challenge lab in the CASIC building, Auburn University. Before challenge, the *F. columnare* bacteria (BGFS-27; genomovar II) [26] were cultured from a single colony and re-isolated from a symptomatic fish. The bacteria were inoculated in modified Shieh broth and grown in the shaker incubator (100 rpm) for 24 h at 28 °C. Challenge experiments were conducted by immersion exposure for 2 h at a final concentration 1×10^5 CFU/mL. After eight weeks of the above feeding regimen, fish from 3 replicate per treatment were challenged with *F. columnare* through standard bath challenge [10,22]. Daily and accumulative mortality was tracked to preliminarily estimate the effect of four diets.

At nine weeks, based on pre-challenge trial results, basal, B + Actigen®, and B + Allzyme® SSF groups were selected for further challenges with *F. columnare*. Four tanks were used for each group, three of which were challenged with *F. columnare* and one

Table 1
Composition (g/100 g as is) of test diets formulated to contain 36% protein and 8% lipids for the evaluation of two dietary supplements.

Ingredient	Basal (B)	B + Allzyme® SSF	B + Actigen®	B + Allzyme® SSF + Actigen®
Fishmeal[a]	6.00	6.00	6.00	6.00
Soybean meal[b]	60.00	60.00	60.00	60.00
Corn gluten meal[c]	5.00	5.00	5.00	5.00
Corn, yellow[d]	18.00	18.00	18.00	18.00
Corn starch[e]	0.84	0.79	0.74	0.69
Menhaden Fish Oil[a]	5.56	5.56	5.56	5.56
Vitamin premix[f]	1.80	1.80	1.80	1.80
Choline chloride	0.20	0.20	0.20	0.20
Stay C 25%[g]	0.10	0.10	0.10	0.10
Trace mineral premix[h]	0.50	0.50	0.50	0.50
CaP-dibasic[e]	2.00	2.00	2.00	2.00
Allzyme® SSF[i]	0.00	0.05	0.00	0.05
Actigen®[i]	0.00	0.00	0.10	0.10

[a] Omega Protein Inc., Reedville, VA, USA.
[b] De-hulled solvent extract soybean meal, Bunge Limited, Decatur, AL, USA.
[c] Empyreal® 75, Cargill Corn Milling, Cargill, Inc., Blair, NE, USA.
[d] Faithway Feed Co., Guntersville, AL, USA.
[e] MP Biochemicals Inc., Solon, OH, USA.
[f] Vitamin (g/kg Premix): Thiamin HCl 0.44, Riboflavin 0.63, Pyridoxine HCl 0.91, D pantothenic acid 1.72, Nicotinic acid 4.58, Biotin 0.21, Folic acid 0.55, Inositol 21.05, Menadione sodium bisulfite 0.89, Vitamin A acetate (500,000 IU g^{-1}) 0.68, Vitamin D_3 (400,000 IU g^{-1}) 0.12, DL-alpha-tocoperol acetate (250 IU g^{-1}) 12.63, cellulose 955.59.
[g] Stay-C® (L-ascorbyl-2-polyphosphate), Roche Vitamins Inc., Parsippany, NJ, USA.
[h] Trace mineral (g/100 g Premix): Cobalt chloride 0.004, Cupric sulfate pentahydrate 0.25, Ferrous sulfate 4.0, Magnesium sulfate anhydrous 13.862, Manganous sulfate monohydrate 0.65, Potassium iodide 0.067, Sodium selenite 0.01, Zinc sulfate hepahydrate 13.193, cellulose 67.964.
[i] Alltech Inc., Nicholasville, KY, USA.

tank served as the control group. Control fish were treated with identical procedures except that they were not exposed to the bacteria, but exposed to sterile modified Shieh broth. Gill, skin, and intestine tissues were collected before (0 h) and soon after challenge (1 h, 2 h, 8 h). Equal amounts of tissue (approximately 50 mg) were collected from each fish within the three pools (3 pools of 5 fish each). The fish were euthanized with tricaine methanesulfonate (MS 222) at 300 mg/L (buffered with sodium bicarbonate) before tissues were collected. Pooled tissues were put into 5 ml RNALater™ at −80 °C until RNA extraction. The remaining challenged catfish were utilized to monitor challenge mortality in 9–60 L (45 L water) aquaria (3 aquaria/diet, 25 fish/aquaria) every 8 h with flow through water as previously described [27]. Median days to death and survival rate at the end of process were recorded. Survival data was analyzed with SigmaPlot 11 (San Jose, CA, USA) using Kaplan–Meier Log Rank Survival Analysis and all pair-wise multiple comparisons used the Holm-Sidak method with adjusted *P* values. Treatment effects were considered significant at $P < 0.05$ [22].

2.3. RNA extraction, library construction and sequencing

Based on the results of median days to death, survival rate and overall response against columnaris, we carried out transcriptomic comparison of gene expression of fish fed with the B + Actigen® diet and the basal diet before (0 h) and after (8 h) columnaris challenge using high-throughput RNA-seq (2 diets × 2 timepoints × 3 replicates = 12 samples). Total RNA extraction was carried out following the manufacturer's directions using the RNeasy Plus Universal Mini Kit (Qiagen). RNA quality of each sample was measured on an Agilent 2100 Bioanalyzer using the RNA Nano Bioanalysis chip. RNA-seq library preparation was carried out by HudsonAlpha Genomic Services Lab (Huntsville, AL, USA). Briefly, cDNA libraries were prepared with 2.14–3.25 μg of starting total RNA and using the Illumina TruSeq RNA Sample Preparation Kit (Illumina), as dictated by the TruSeq protocol. The libraries were amplified with 15 cycles of PCR and contained TruSeq indexes within the adaptors, specifically indexes 1–12. Finally, amplified library yields were 30 μg of 19.8–21.4 ng/μl with an average length of ~270 bp, indicating a concentration of 110–140 nM. 12 samples were clustered per lane and sequenced by an Illumina HiSeq 2000 instrument with 100 bp paired end (PE) reads.

2.4. De novo assembly and annotation

De novo assembly of sequencing reads by Trinity package was applied after raw reads trimming [28]. Before assembly, raw reads were trimmed by removing adaptor sequences and ambiguous nucleotides. Reads with quality scores less than 20 and length below 30 bp were all trimmed. High quality sequences were then assembled based on three independent software modules. Inchworm assembled raw reads into unique transcripts by kmers (k-mer 25) and computed their abundance values. Chrysalis merged identified contigs from Inchworm into de Bruijn graphs. Butterfly traced the paths that reads and pairs of reads taken within the graph and reported full-length transcripts as well as paralogous genes [29]. The assembled contigs were used as queries against the NCBI zebrafish protein database, the UniProtKB/SwissProt database and the non-redundant (NR) protein database using the BLASTX program. The cutoff E-value was set at 1e-5 and only the top gene id and name were initially assigned to each contig.

2.5. Identification of differentially expressed contigs

The high quality reads from each sample were mapped onto the Trinity reference assembly using CLC Genomics Workbench software. At least (95%) of the read length was required to align to the reference and a maximum of two mismatches were allowed during mapping. The total mapped reads number for each transcript was determined, and then normalized to detect RPKM (Reads Per Kilobase of transcript per Million mapped reads). The proportions-based Baggerly's test was used to identify the differentially expressed genes between Actigen®-fed and basal-fed fish at two timepoints with FDR corrected $P < 0.05$ [30]. The fold changes were calculated after scaling normalization of the RPKM values [31]. Analysis was performed using the RNA-seq module and the expression analysis module in CLC Genomics Workbench.

Transcripts with absolute fold change values larger than 2 were included in analysis as the differentially expressed genes.

Contigs with previously identified gene matches were carried forward for further analysis. Functional groups and pathways encompassing the differently expressed genes were identified based on GO analysis, pathway analysis based on the Kyoto Encyclopedia of Genes and Genomes (KEGG) database, and manual literature review.

2.6. Gene ontology and enrichment analysis

In order to identify overrepresented GO annotations in the differentially expressed gene set compared to the broader reference assembly, GO analysis and enrichment analysis of significantly expressed GO terms was performed using Ontologizer 2.1 using the Parent-Child-Intersection method with a Benjamini-Hochberg multiple testing correction [32,33]. GO terms for each gene were obtained by utilizing zebrafish annotations for the unigene set. The difference of the frequency of assignment of gene ontology terms in the differentially expressed genes sets were compared to the overall catfish reference assembly. The threshold was set as FDR corrected $P < 0.05$.

2.7. Experimental validation: QPCR

A total of 10 differentially expressed genes were selected for validation using real time QPCR with gene specific primers designed using Primer3 software based on RNA-seq contig sequences (Table 2). Total RNA was extracted using the RNeasy Plus Universal Mini Kit (Qiagen) following manufacturer's instructions. First strand cDNA was synthesized by qScript™ cDNA Synthesis Kit (Quanta BioSciences) according to manufacturer's protocol. The qScript chemistry used a blend of oligo-dT and random primers. All the cDNA products were diluted to 250 ng/μl and utilized for the quantitative real time PCR reaction using the PerfeCTa® SYBR® Green FastMix® (Quanta BioSciences, Gaithersburg, MD, USA) on a CFX96 real-time PCR Detection System (Bio-Rad Laboratories, Hercules, CA, USA). The thermal cycling profile consisted of an initial denaturation at 95 °C (for 30 s), followed by 40 cycles of denaturation at 94 °C (5 s), an appropriate annealing/extension temperature (58 °C, 5 s). An additional temperature ramping step was utilized to produce melting curves of the reaction from 65 °C to 95 °C. Results were expressed relative to the expression levels of 18S rRNA in each sample using the Relative Expression Software Tool (REST) version 2009 [34]. The biological replicate fluorescence intensities of the control and treatment products for each gene, as measured by crossing-point [35] values, were compared and converted to fold change by the relative quantification method. The mathematical model was based on the correction for PCR efficiencies (assumed as 2) and the mean crossing point (Ct) deviation between sample groups and control groups. Expression differences between groups were assessed for statistical significance using a randomization test (≥2000 randomizations) and plotted using standard error (SE) estimation. Test amplifications were conducted to ensure that 18S and target genes were within an acceptable range. A no-template control was run on all plates. QPCR analysis was repeated in triplicate runs (technical replicates) to confirm expression patterns.

3. Results

3.1. Catfish feed trial and challenge

Diets were formulated according to a standard catfish diet with the addition of Actigen®, Allzyme® SSF, or both products. Channel catfish fingerlings were fed from a 4.1 g average starting weight for nine weeks. All groups showed good weight gain, feed conversion ratios (FCRs) below 1.0, and excellent survival (>95%). No significant differences in growth, FCR, or survival were observed among the different diet treatments (Table 3).

Following a pre-challenge of a subset of the fed fingerlings (data not shown), the basal, Actigen®, and Allzyme® SSF groups were chosen for a full challenge to examine potential differences in *F. columnare* susceptibility. We challenged with a virulent *F. columnare* isolate known to cause heavy mortalities by two days in aquaculture settings. While mortality levels exceeded expectations based on pre-challenge dosage, there were statistically significant differences in survival curves of all three groups (Fig 1; $P < 0.001$). Mean survival times were 2.0, 2.5, and 5.0 days with the basal, Allzyme® SSF, and Actigen® diets respectively. Inclusion of Actigen® significantly enhanced survival, with 32% of challenged fish from that dietary treatment surviving at the completion of the challenge period compared with 100% mortality in the other two treatments.

3.2. Sequencing and assembly

Given the clear protective effect of the Actigen®-supplemented diet, we chose to compare the whole transcriptome expression between the basal and Actigen® diet at 0 h and 8 h post infection. The 8 h post infection timepoint has been previously shown to be a key timepoint for pathogen adherence as well as a point where we have observed diverging immune responses between resistant and susceptible catfish [10,22]. Three replicate samples were used for each treatment/timepoint for a total of 12 samples. Approximately 40 million reads were obtained for each of the twelve libraries. After removing ambiguous nucleotides, low-quality sequences (quality scores < 20) and short reads (length < 30 bp), the

Table 2
Primers used for QPCR validation (5′ to 3′).

Gene	Forward	Reverse
Anterior gradient protein 2 homolog	TCCTTCTTGACCGCAGTCTTGT	AACCTGAGAGCAGCCTGTGAA
Argininosuccinate synthase	GTCTATAACAGGTGATGGACAG	GACACGTAGGAGCATTATATCC
Caspase-1-like, partial	ATTTTGTGTCTGACGGGCTA	GGCCCACAAAGTGATAGAAG
CC chemokine 106 SCYA106	CATTGGACTGCTGTTTGAAG	TTTTCATCAGCTCTCTGACC
CC chemokine 109 SCYA109	CTGAACTTTCTACAGTGTGTGG	GAACTGAAGAACTGGAGAGGA
IgGFc-binding protein-like isoform X1	AGTCACCAACTTGGAAAGAG	CCTCGCTTCAAATGTATCCT
Interleukin 17a/f1 precursor	TGGTTGCTCAGGCTGCTCCTT	ACGCCAGCTTGATGTCATGTTCC
Interleukin-1 beta	AGGCTTAGAGGAGGTAAAAGAC	CTTATAGTCCTCCTTTGAGGTG
Matrix metalloproteinase-9 precursor	GTGCGCTACTACAGCCAAT	TCGTGCAGGAAGTATAGGTT
Rhamnose binding lectin type Ia	GTGATGTCCAAAGACTCACGTG	GGTCGGGGTTGCCAAGTAAATC
Toxin-1 precursor	CTGCCTAGAAACTTCTGGTGT	CCAGGTCTCTTACAGAACTCC
18S rRNA	GAGAAACGGCTACCACATCC	GATACGCTCATTCCGATTACAG

Table 3
Aquaria-based growth and survival response of juvenile channel catfish (average size 4.1 ± 0.11 g) to the test diets over an eight week growth trial.

Treatments	Final mean weight (g)	Mean weight Gain (%)	FCR	Survival (%)
Basal	35.01	754.60	0.79	96.67
B + Allzyme® SSF	32.03	692.90	0.83	97.78
B + Actigen®	34.27	745.30	0.82	98.89
B + Allzyme® SSF + Actigen®	34.02	747.80	0.82	95.00
PSE[a]	0.80	19.21	0.02	1.61
P-Value	0.08	0.11	0.40	0.38

[a] Pooled Standard Error.

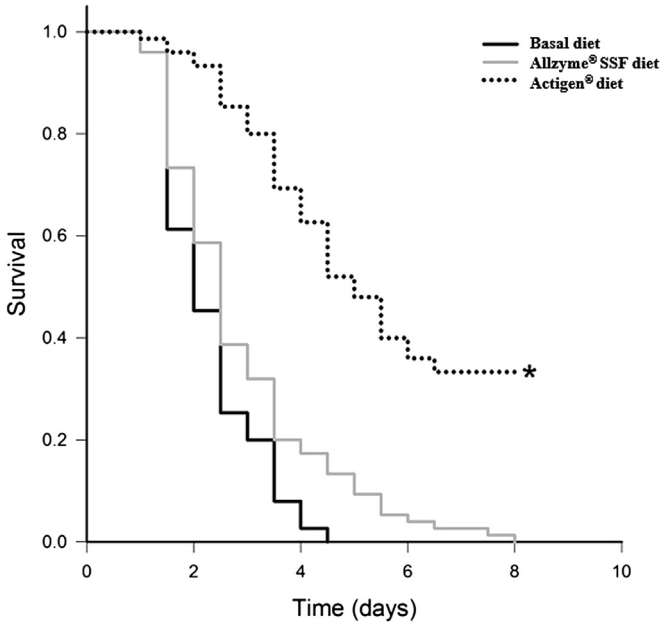

Fig. 1. Summary of cumulative survival rate of channel catfish fingerlings after challenge with virulent *F. columnare* ($P < 0.001$).

Table 4
Summary of *de novo* assembly results of Illumina RNA sequence data from channel catfish gill using Trinity assembler.

Contigs	396,019
Large contigs (1000 bp)	88,311
N50 (bp)	1411
Median contig length	413
Average contig length	798
Reads mapped in pairs (%)	67.84%

Table 5
Summary of gene identification and annotation of assembled catfish contigs based on BLAST homology searches against various protein databases (Zebrafish, UniProt, NR). Putative gene matches were at E-value ≤ 1e-5. Hypothetical gene matches denote those BLAST hits with uninformative annotation. Quality unigene hits denote more stringent parameters, including score ≥ 100, E-value ≤ 1e-20.

	Channel catfish		
	Zebrafish	UniProt	NR
Contigs with gene matches	103,692	95,179	112,104
Annotated contigs ≥ 500 bp	56,819	79,036	88,634
Annotated contigs ≥ 1000 bp	22,281	61,745	66,636
Unigene matches	24,636	28,833	36,631
Hypothetical gene matches	2024	0	3320
Quality unigene matches	15,096	17,049	23,689

remaining high-quality reads were carried forward for assembly and analysis. The Trinity assembly generated 396,019 contigs with average length of 798 bp, N50 size of 1411 bp in its initial assembly, and 88,311 contigs longer than 1000 bp (Table 4). Raw read data are archived at the NCBI Sequence Read Archive (SRA) under Accession SRP052919 (http://www.ncbi.nlm.nih.gov/sra/?term=SRP020252).

3.3. Gene identification and annotation

BLAST-based gene identification was performed to annotate the transcriptome and inform downstream differential expression analysis. After gene annotation, 112,104 Trinity contigs had a significant BLAST hit against 36,631 unique non-redundant genes. 23,689 unigenes were identified based on hits to the NR database with the more stringent criteria of a BLAST score ≥ 100 and E-value ≤ 1e-20. The same BLAST criteria were used in comparison of the Trinity reference contigs with the Uni-Prot and zebrafish database (Table 5). Direct comparison of expression levels between basal and Actigen® enhanced diets at 0 h (pre-challenge) revealed a relatively small (148) number of differentially expressed genes. In contrast, direct comparison of 8 h (post-challenge) expression differences, revealed 3042 differentially expressed genes with over 96% of those showing higher expression in the Actigen® diet treatment relative to the basal diet treatment (Table 6; Supplementary Table 1).

3.4. Enrichment and pathway analysis

Differentially expressed unique genes were used as inputs to perform enrichment analysis using Ontologizer 2.1. Terms with $P < 0.05$ (FDR-corrected) were considered significantly over-represented. Ten higher level GO terms for each comparison (within group and between group) were retained as informative for further pathway analysis (Table 7). Enriched GO terms highlighted processes and pathways evident from the differentially expressed gene sets including broadly differing immune responses between dietary treatments, profound dysregulation of extracellular matrix components, and changes in mucosal constituents likely governing the rate of pathogen adhesion and colonization. Differentially expressed genes representing these signatures were gathered (Table 8) from the larger dataset (Supplementary Table 1) and the putative functional significance of their differential expression is discussed below.

Table 6
Statistics of differentially expressed genes following *F. columnare* challenge between Actigen® and basal diet treated fish at 0 h and 8 h. Values indicate contigs/genes passing cutoff values of fold change ≥ 2 (FDR-corrected $P < 0.05$).

Group	Up-regulated	Down-regulated	Total
Basal diet 8 h vs 0 h	178	213	391
Actigen® diet 8 h vs 0 h	990	22	1012
Actigen® vs Basal 0 h	120	28	148
Actigen® vs Basal 8 h	2932	110	3042

Table 7
Summary of GO term enrichment results of significantly expressed genes in channel catfish between dietary treatments. The differentially expressed genes were analyzed as the study set in analyzing terms in within-group comparison of Basal (A) and Actigen® (B) treatments, and between-group comparison of 0 h (pre-challenge, C) and 8 h (post-challenge, D). FDR correct $P \leq 0.05$ was considered significant. Population count is the number of genes associated with the term in the population set. Study count is the number of genes associated with the term in the study set. GO names were retained only from GO terms of levels >2.

GO ID	GO name	p-Value(FDR)	Population count	Study count
A				
GO:0050896	Response to stimulus	4.91E-07	2673	89
GO:0005581	Collagen trimer	2.48E-06	44	8
GO:0009607	Response to biotic stimulus	5.33E-05	111	13
GO:0002376	Immune system process	6.58E-05	419	22
GO:0042611	MHC protein complex	0.000197	14	4
GO:0005201	Extracellular matrix structural constituent	0.000336	29	6
GO:0005102	Receptor binding	0.001571	345	17
GO:0034097	Response to cytokine	0.002278	56	6
GO:0050839	Cell adhesion molecule binding	0.002298	24	4
GO:0005539	Gycosaminoglycan binding	0.004857	44	5
B				
GO:0032502	Developmental process	8.97E-13	2406	204
GO:0032501	Multicellular organismal process	4.07E-10	2351	191
GO:0022610	Biological adhesion	7.19E-10	261	41
GO:0065007	Biological regulation	2.38E-06	1225	101
GO:0005856	Cytoskeleton	2.54E-06	3897	265
GO:0005201	Extracellular matrix structural constituent	3.07E-06	526	47
GO:0006793	Phosphorus metabolic process	2.03E-05	29	9
GO:0043412	Macromolecule modification	2.20E-05	1303	105
GO:0050896	Response to stimulus	7.06E-05	2673	186
GO:0097367	Carbohydrate derivative binding	0.000555	1450	124
C				
GO:0043062	Extracellular structure organization	0.002692	35	3
GO:1901699	Cellular response to nitrogen compound	0.003096	51	4
GO:0006955	Immune response	0.003401	182	6
GO:1901698	Response to nitrogen compound	0.008329	82	4
GO:0018193	Peptidyl-amino acid modification	0.010728	171	6
GO:0007167	Enzyme linked receptor protein signaling pathway	0.012131	288	7
GO:0008283	Cell proliferation	0.020587	190	5
GO:0006952	Defense response	0.028256	133	5
GO:0018212	Peptidyl-tyrosine modification	0.029928	41	4
GO:0004055	Argininosuccinate synthase activity	0.036036	1	1
D				
GO:0065007	Biological regulation	3.03E-11	3897	743
GO:0022610	Biological adhesion	6.97E-10	261	81
GO:0006793	Phosphorus metabolic process	2.14E-09	1225	282
GO:0097367	Carbohydrate derivative binding	1.71E-08	1450	335
GO:0050896	Response to stimulus	1.02E-06	2673	507
GO:0044271	Cellular nitrogen compound biosynthetic process	2.53E-06	1408	275
GO:0005201	Extracellular matrix structural constituent	8.07E-06	29	14
GO:0005581	Collagen trimer	0.000139	44	17
GO:0043412	Macromolecule modification	0.000158	1303	269
GO:0009611	Response to wounding	0.000737	175	46

3.5. Validation of RNA-seq profiles by QPCR

For validation of differentially expressed genes identified from this study and previous RNA-seq, we selected 10 genes for QPCR confirmation, choosing from those with different expression patterns and from genes of interest based on functional enrichment and pathway results. Expression changes in these genes by QPCR were significantly correlated with those shown by RNA-seq ($R = 0.88$; Fig 2), indicating that while absolute degree of expression change of the two methods can be different, the patterns and general magnitude of expression change captured by RNA-seq were largely accurate.

One key aspect of the expression patterns of particular interest to us based on previous findings was the divergent patterns of rhamnose binding lectin 1a (RBL) between the basal control diet and the Actigen®-enriched diet. Previously, we have shown that higher RBL expression in catfish is linked to greater susceptibility to acute columnaris outbreaks [22]. While RBL1a was identified from sequenced contigs, it was not found to be differentially expressed by RNA-seq analysis. However, additional QPCR analysis of expression at 1 h and 2 h, as well as 8 h, showed that while both dietary treatments upregulated RBL at 1 h post-challenge, expression levels dropped dramatically by 2 h and continued to decline to 8 h in the Actigen® treatment, while they remained significantly higher in the control diet (Fig 3). These patterns closely mimic those previously observed in catfish resistant and susceptible to columnaris [4]. The RNA-seq assembly process may have merged reads from both RB1a and the highly similar RBL1b [24], masking differences at 8 h, whereas QPCR primers were designed to only amplify RBL1a.

4. Discussion

Our understanding of dietary-driven protection of surface mucosa has been limited. However, the gill, skin, and nares of fish are critically important routes of infection [36]. Recent research, for example, has revealed the importance of nasal surfaces in trout as routes of infection and vaccination [37]. Work by our group has previously shown the critical interaction between nutritional status (fasted vs fed) and immunity in the skin and gill of channel catfish

Table 8
Differentially expressed genes in the gill between Actigen® and basal-fed channel catfish in different functional classifications. Positive values indicate higher expression at Actigen® treatment while negative values indicate higher expression at Basal treatment. Bold values indicate a significant fold change (FDR-corrected $P < 0.05$).

Description	Feature ID	Actigen® vs basal		Basal	Actigen®
		Between group		Within group	
		0 h	8 h	8 h vs 0 h	
IL4R pathway					
E3 ubiquitin-protein ligase CBL	c78522_g4_i2	2.59	**6.88**	1.16	**3.09**
Growth factor receptor-bound protein 10 isoform X3	c76466_g4_i3	1.03	**9.50**	−1.86	4.82
Insulin receptor substrate 1-B-like isoform X2	c80575_g6_i2	1.54	**3.80**	−1.03	2.40
Insulin receptor substrate 2	c82722_g12_i1	1.12	**3.44**	−1.30	**2.34**
Interleukin-4 receptor subunit alpha isoform X3	c81765_g4_i1	**2.15**	1.85	1.81	1.55
Janus kinase 3	c77974_g4_i5	**2.11**	**2.03**	1.51	1.44
Mitogen-activated protein kinase 3	c78210_g10_i3	1.51	**2.96**	1.00	1.98
Protein tyrosine phosphatase, non-receptor type 11	c75032_g3_i4	1.38	**3.78**	−1.41	1.98
Proto-oncogene c-Fos-like	c70011_g1_i2	1.43	**6.48**	**−5.28**	−1.15
Signal transducer and activator of transcription 3 isoform	c78505_g14_i6	1.25	**2.76**	−1.10	**2.00**
Signal transducer and activator of transcription 5	c82916_g2_i3	1.84	**3.36**	1.19	**2.20**
Signal transducer and activator of transcription 5b	c82916_g2_i6	1.42	**3.67**	−1.32	1.94
Signal transducer and activator of transcription 6	c79892_g8_i11	2.40	**5.13**	1.49	**3.10**
Son of sevenless homolog 1-like isoform X1	c82956_g11_i6	1.37	**7.83**	−1.12	5.01
Immune/inflammatory response					
Argininosuccinate synthase	c82175_g7_i2	**2.05**	1.09	**2.55**	1.36
Caspase-1-A-like	c71179_g1_i1	4.47	−2.52	**9.34**	−1.20
Caspase-1-like, partial	c197216_g1_i1	**−7.46**	**−3.66**	**−2.71**	−1.32
C–C chemokine receptor type 7-like	c71752_g1_i2	**2.25**	1.25	**2.33**	1.29
CC chemokine SCYA106	c78989_g3_i3	2.42	−1.50	**4.70**	1.30
CC chemokine SCYA109	c77257_g5_i3	2.99	**−2.94**	**8.84**	1.02
CC chemokine SCYA113	c74352_g3_i4	6.04	−2.33	**14.10**	−1.00
CC chemokine SCYA116	c70509_g1_i1	**3.71**	−1.45	**6.58**	1.22
CD209 antigen-like protein 2-like isoform X1(DC-SIGN)	c75853_g2_i11	**−5.56**	−2.00	**−2.86**	−1.03
CD4-like protein 1	c77482_g1_i2	2.66	−1.12	**3.38**	1.11
CD4-like protein 2 precursor	c76656_g2_i4	2.23	1.11	**3.10**	1.57
Chemokine (C-X-C motif) ligand 12b (stromal cell-derived factor 1)	c79153_g4_i4	−1.32	**3.88**	**−2.11**	**2.44**
Complement C1q tumor necrosis factor-related protein	c76437_g11_i2	1.04	**5.08**	−1.83	**2.72**
Complement C4-1	c83218_g2_i10	1.70	**2.81**	1.34	2.13
Connector enhancer of kinase suppressor of ras 3-like	c79400_g2_i1	1.81	**3.25**	1.19	**2.22**
C-type lysozyme	c64942_g1_i2	**2.71**	−1.03	2.75	−1.01
C-type mannose receptor 2	c79310_g5_i3	1.22	**6.91**	−1.74	**3.31**
C-X-C motif chemokine 10-like	c78829_g1_i5	2.77	−1.39	**4.80**	1.27
Galectin-4	c78285_g4_i1	11.26	**121.89**	−1.99	**5.59**
Galectin-4-like, partial	c78285_g2_i4	1.44	**11.67**	−2.30	3.23
Ig kappa chain V–III region CLL precursor	c83593_g1_i1	3.70	−1.34	**4.20**	−1.22
Ig mu chain C region membrane-bound form	c81635_g1_i5	1.93	−1.36	**2.98**	1.12
IgGFc-binding protein-like	c76549_g1_i1	4.11	**22.12**	−1.24	**5.25**
Immunoglobulin light chain	c83492_g3_i4	2.07	−1.30	**2.59**	−1.04
Integrin alpha 6b precursor	c83435_g3_i6	1.44	**4.69**	−1.37	**2.38**
Integrin alpha-1	c83443_g8_i4	1.92	**6.90**	−1.39	**2.58**
Integrin alpha-10 isoform X1	c82839_g3_i3	1.50	**7.11**	−1.79	2.40
Integrin alpha-2-like	c82135_g3_i11	1.55	**5.96**	−1.47	**2.63**
Integrin alpha-3 isoform X2	c78267_g4_i1	1.91	**6.71**	−1.13	**3.12**
Integrin alpha-3-like	c78267_g4_i2	2.48	**3.58**	1.95	2.85
Integrin alpha-5 precursor	c79286_g3_i8	1.51	**5.25**	−1.40	**2.49**
Integrin alpha-8	c80757_g25_i1	1.02	**2.16**	−1.33	1.57
Integrin alpha-E-like (CD103)	c80604_g3_i2	**2.67**	1.80	2.34	1.55
Integrin alpha-X-like	c84227_g2_i5	1.60	**3.10**	1.30	2.48
Integrin beta-3-like	c79865_g3_i1	1.12	**3.04**	−1.21	2.20
Integrin beta-4 isoform X1	c81949_g1_i7	2.08	**9.13**	−1.81	**2.45**
Integrin beta-4 isoform X2	c81949_g1_i6	1.41	**5.31**	−1.72	**2.18**
Integrin beta-7-like	c76232_g7_i4	2.31	**2.68**	1.72	**2.03**
Integrin, beta 1	c80193_g4_i4	1.11	**5.10**	**−2.34**	1.99
Interleukin 1, beta	c78925_g2_i12	1.37	6.94	**−7.01**	−1.38
Interleukin 17a/f1 precursor	c77837_g8_i2	23.42	−2.33	**67.92**	1.21
Interleukin 17a/f2 precursor	c62007_g1_i1	8.30	−1.51	**37.83**	2.92
Interleukin 22	c70125_g2_i1	7.81	−1.11	**11.16**	1.32
Interleukin 7 receptor precursor	c78110_g5_i1	1.63	**3.24**	1.41	**2.81**
Interleukin-1 receptor type 1-like	c82485_g5_i9	1.73	**10.10**	−2.54	2.36
Interleukin-11 receptor subunit alpha isoform X1	c80717_g11_i10	1.30	**12.32**	−1.88	**4.94**
Interleukin-13 receptor subunit alpha-2 precursor	c77237_g2_i3	1.56	−1.36	**2.43**	1.14
Interleukin-6 receptor subunit beta	c81756_g1_i6	1.58	**4.64**	−1.27	**2.31**
Interleukin-6 receptor subunit beta-like isoform X1	c78102_g6_i2	1.46	**3.70**	−1.11	**2.38**
Kinase suppressor of Ras 1-like isoform X2	c78509_g6_i3	4.71	**7.52**	1.44	2.26
Lymphocyte antigen 75 (DEC205)	c83066_g2_i1	**2.60**	**8.31**	−1.08	**2.95**
Macrophage mannose receptor 1	c80828_g1_i2	1.19	**2.61**	1.08	**2.35**
MHC class II beta chain, partial	c77410_g5_i3	1.86	−1.63	**3.76**	1.24
MHC class IIA antigen	c79083_g6_i3	2.17	−1.11	**4.14**	1.70

Table 8 (*continued*)

Description	Feature ID	Actigen® vs basal		Basal	Actigen®
		Between group		Within group	
		0 h	8 h	8 h vs 0 h	
Microfibril-associated glycoprotein 4-like isoform X1	c80625_g2_i2	1.51	**−2.58**	**4.11**	1.05
N-acetylglutamate synthase, mitochondrial-like	c84176_g5_i2	1.33	**2.11**	−1.18	1.35
Natterin-like protein	c83837_g6_i3	1.42	**4.48**	**−3.70**	−1.20
Olfactomedin-like 3	c76681_g3_i3	**−3.92**	1.04	**−3.39**	1.24
Ornithine aminotransferase, mitochondrial	c82495_g10_i1	1.66	**3.93**	−1.18	**2.01**
Protein jagged-2-like isoform X2	c82047_g5_i2	−1.02	**3.71**	−1.31	2.79
Protein NLRC3-like isoform X1	c78545_g4_i3	2.35	**16.72**	−2.15	**3.49**
Protein NLRC5	c78312_g1_i1	2.90	**4.33**	1.82	**2.66**
Protein NLRC5-like	c82299_g2_i1	**2.20**	**2.88**	1.28	1.68
Retinoic acid receptor gamma-A	c78386_g8_i14	1.44	**2.24**	1.02	1.58
Retinoic acid receptor gamma-A-like isoform X2	c70458_g2_i1	8.21	**60.23**	−4.02	2.39
Secretory phospholipase A2 receptor	c79169_g6_i2	1.31	**8.82**	−1.63	**4.04**
T cell receptor alpha, partial	c83360_g3_i2	2.77	−1.77	**3.22**	−1.54
T cell receptor gamma 2	c77668_g3_i1	2.39	−1.79	**3.14**	−1.32
T-cell antigen receptor alpha, partial	c83360_g3_i3	2.37	−1.47	**3.62**	1.04
T-cell antigen receptor beta	c80911_g1_i7	1.92	−1.65	**3.26**	1.03
Tight junction protein ZO-1-like isoform X10	c76166_g6_i2	1.89	**4.38**	1.02	**2.35**
Tight junction protein ZO-1-like isoform X2	c81503_g3_i5	1.65	**10.08**	−1.26	**4.70**
Tight junction protein ZO-3-like isoform X2	c83258_g4_i4	**2.04**	**4.68**	−1.08	**2.12**
Toxin-1 precursor	c82831_g4_i1	−1.19	2.08	**−3.04**	−1.23
Transforming growth factor, beta 1a precursor	c81254_g6_i2	1.11	**3.32**	−1.41	**2.12**
Tumor necrosis factor receptor superfamily member 14	c81448_g3_i2	**10.29**	2.40	5.55	1.31
ECM/Tissue repair/Resolution					
A disintegrin and metalloproteinase with thrombospondin motifs 10	c78926_g3_i3	2.25	**6.05**	1.37	3.77
Cathepsin K	c71256_g1_i3	−1.58	1.13	**2.76**	1.55
Chitinase-like protein PB1E7.04c-like	c77776_g5_i2	2.79	**15.71**	−1.63	**3.49**
Collagen alpha-1(II) chain-like isoform X2	c82454_g8_i2	−1.19	**5.96**	**−3.13**	2.26
Collagen alpha-1(IX) chain-like	c81123_g1_i2	−1.38	**2.86**	−2.37	1.66
Collagen alpha-1(VI) chain	c79446_g1_i2	−1.17	**3.08**	**−2.08**	1.73
Collagen alpha-1(X) chain-like	c78022_g2_i1	−1.72	**2.75**	**−3.07**	1.54
Collagen alpha-1(XI) chain isoform X1	c84151_g2_i1	1.02	**7.24**	**−2.73**	**2.55**
Collagen alpha-1(XI) chain isoform X5	c84151_g2_i7	−1.38	**2.60**	**−2.44**	1.47
Collagen alpha-1(XI) chain-like	c83057_g1_i7	1.03	**3.60**	−1.76	1.98
Collagen alpha-1(XI) chain-like isoform X6	c80532_g3_i16	1.21	**7.82**	−2.57	**2.56**
Collagen alpha-1(XII) chain isoform X1	c77224_g7_i6	1.04	**13.08**	**−3.32**	**3.72**
Collagen alpha-1(XII) chain-like isoform X2	c82683_g7_i11	−1.06	**3.46**	−1.96	1.87
Collagen alpha-1(XII) chain-like isoform X3	c77224_g5_i3	1.97	**50.72**	−2.65	**8.46**
Collagen alpha-1(XII) chain-like isoform X4	c77224_g7_i3	1.86	**45.89**	−2.08	**11.65**
Collagen alpha-1(XII) chain-like isoform X5	c77224_g5_i1	1.52	**27.77**	−2.48	**7.56**
Collagen alpha-1(XIV) chain	c77222_g1_i3	1.03	**4.23**	−1.79	2.18
Collagen alpha-1(XVI) chain-like	c82903_g6_i8	−1.22	**4.59**	−2.17	**2.60**
Collagen alpha-1(XVIII) chain-like isoform X2	c81631_g7_i9	1.10	**8.06**	−2.55	**2.97**
Collagen alpha-1(XVIII) chain-like isoform X3	c81631_g7_i4	1.38	**2.92**	1.15	**2.39**
Collagen alpha-1(XXII) chain precursor	c77456_g2_i6	1.50	**16.19**	−5.68	1.96
Collagen alpha-1(XXIII) chain-like	c78447_g11_i5	−1.07	**2.71**	−1.93	1.55
Collagen alpha-1(XXVII) chain B precursor	c80585_g3_i8	1.37	**8.89**	−1.24	**5.13**
Collagen alpha-2(IV) chain isoform X2	c82843_g3_i2	1.15	**2.05**	−1.18	1.51
Collagen alpha-2(V) chain-like	c75359_g3_i4	−1.07	**3.62**	−2.12	1.83
Collagen alpha-2(VI) chain isoform X2	c79746_g5_i5	−1.20	**2.12**	−1.63	1.56
Collagen alpha-2(VI) chain-like	c79746_g5_i1	−1.40	**3.69**	**−3.30**	1.59
Collagen alpha-2(XI) chain isoform X9	c80532_g3_i7	1.17	**11.25**	−2.85	3.39
Collagen alpha-3(VI) chain-like	c84294_g1_i2	1.38	**5.10**	−1.35	**2.77**
Collagen alpha-4(IV) chain-like	c81110_g2_i5	1.04	**5.03**	−1.17	**4.14**
Collagen alpha-5(IV) chain	c84125_g1_i14	−1.31	**2.82**	**−2.20**	1.68
Collagen alpha-6(IV) chain	c77834_g7_i1	−1.12	**2.01**	−1.66	1.37
Collagen type I alpha 2	c83429_g1_i12	−1.62	**5.34**	**−4.13**	2.10
Collagen type IV alpha 1 precursor	c77834_g9_i4	−1.05	**5.94**	−1.80	**3.50**
Collagen type IV alpha-3-binding protein-like isoform X1	c77391_g9_i3	−1.02	**2.10**	−1.46	1.48
Collagen, type I, alpha 1	c76517_g9_i4	−1.26	**9.15**	**−4.45**	**2.58**
Decorin	c81816_g5_i2	1.09	**5.83**	−2.16	**2.50**
Disintegrin and metalloproteinase domain-containing protein 12	c75507_g3_i1	1.19	**5.20**	−1.89	2.19
Fibronectin	c84233_g5_i9	1.38	**4.00**	−1.43	**2.05**
Fibronectin 1b	c84233_g5_i3	1.10	**2.16**	−1.12	1.74
Fibronectin type III domain-containing protein 1 isoform	c80599_g1_i7	−1.12	**5.60**	−1.63	3.84
Fibronectin type III domain-containing protein 3B	c76568_g3_i6	1.00	**2.60**	−1.53	1.70
Fibronectin type III domain-containing protein 3B-like	c76568_g3_i3	1.14	**13.11**	−2.98	**3.92**
Fibronectin type-III domain-containing protein 3A isoform	c79826_g17_i6	2.02	**7.05**	1.06	**3.55**
Gelsolin-like	c81531_g3_i2	−1.02	**2.00**	−1.31	1.55
Glucocorticoid receptor isoform X1	c80677_g3_i2	1.74	**6.25**	−1.22	2.69
Lumican isoform X1	c78518_g2_i1	**−4.66**	**4.20**	**−5.17**	3.78
Lysyl oxidase homolog 1-like	c78063_g1_i1	1.31	**8.65**	−2.08	**3.22**

(*continued on next page*)

Table 8 (*continued*)

Description	Feature ID	Actigen® vs basal		Basal	Actigen®
		Between group		Within group	
		0 h	8 h	8 h vs 0 h	
Lysyl oxidase homolog 2A-like	c81461_g3_i3	−1.42	**2.90**	−1.95	2.15
Lysyl oxidase homolog 3-like isoform X1	c78790_g3_i5	−1.49	**4.11**	−2.53	2.32
Lysyl oxidase homolog 4	c81080_g10_i3	−1.52	**2.43**	**−2.58**	1.42
Lysyl oxidase homolog 4-like	c81080_g10_i1	−1.65	**5.34**	−3.98	2.13
Matrix metalloproteinase-9 precursor	c79228_g1_i1	−1.58	**11.26**	**−7.34**	2.45
Matrix metalloproteinase 13	c84067_g2_i5	1.15	**2.68**	**−2.15**	1.09
Matrix metalloproteinase 13 precursor	c84067_g6_i2	2.25	**7.07**	−2.26	1.39
Matrix metalloproteinase-15	c77990_g1_i3	−1.32	**2.12**	−1.75	1.61
Matrix metalloproteinase-15-like	c77990_g1_i2	1.95	**5.16**	−1.05	2.65
Matrix metalloproteinase-16-like isoform X2	c80383_g12_i1	1.58	**7.65**	−1.59	**2.92**
Matrix metalloproteinase-19-like	c78392_g1_i4	1.13	**2.05**	−1.18	1.57
Von Willebrand factor precursor	c83313_g6_i2	−1.12	**2.32**	−1.47	1.77
Mucin secretion and modification					
Anterior gradient protein 2 homolog precursor	c74607_g1_i2	3.33	−1.63	**5.40**	−1.01
Anterior gradient protein 2-like protein	c74607_g1_i1	3.63	−2.66	**6.74**	−1.40
Mucin 17-like protein, partial	c81110_g2_i2	1.51	**3.88**	−1.61	1.65
Mucin-17 isoform X2	c78080_g3_i5	6.13	**40.15**	4.00	**23.06**
Mucin-2-like isoform X2	c75765_g1_i9	**3.26**	**21.90**	−1.72	**3.87**
Mucin-5AC-like	c77449_g2_i4	2.86	**24.77**	1.09	**9.99**
Mucin-5AC-like isoform X1	c83581_g8_i2	1.70	**3.13**	1.14	**2.08**
Normal mucosa of esophagus-specific gene 1 protein-like	c71085_g1_i3	**3.09**	−1.59	**3.68**	−1.34
Glycan-Binding					
Aggrecan core protein isoform X2	c18174_g1_i1	1.58	**14.51**	−1.88	**4.70**
Aggrecan core protein-like	c76196_g1_i3	1.03	**13.10**	−2.67	**4.64**
Amyloid beta A4 precursor protein-binding family B member	c80591_g3_i5	1.75	**3.46**	1.06	**2.10**
Amyloid beta A4 protein isoform X2	c82991_g3_i8	−1.78	**4.22**	**−4.63**	1.62
Amyloid beta A4 protein-like isoform X3	c73051_g3_i3	−1.70	**3.58**	**−2.22**	**2.72**
Amyloid beta precursor protein b	c73051_g1_i1	1.14	**4.75**	−1.55	**2.67**
Chondroitin sulfate N-acetylgalactosaminyltransferase	c74740_g1_i3	1.54	**3.78**	1.08	**2.73**
Chondroitin sulfate proteoglycan 4	c78627_g1_i1	1.21	**8.44**	−1.68	**4.49**
Chondroitin sulfate synthase 1	c76672_g2_i1	1.31	**2.88**	−1.33	1.66
Dermatan-sulfate epimerase isoform X1	c78896_g7_i3	−1.18	**2.82**	−1.75	1.91
Fibroblast growth factor 2-like	c77976_g11_i1	1.78	**3.28**	−1.02	1.82
Fibroblast growth factor 23 precursor	c81950_g3_i1	1.20	**2.88**	−1.89	1.26
Fibroblast growth factor receptor 1-A-like isoform X2	c80308_g6_i5	−1.08	**2.63**	−1.56	1.83
Fibroblast growth factor receptor 2 isoform X3	c84177_g1_i15	−1.43	**3.18**	−2.43	1.94
Fibroblast growth factor receptor 3 isoform X4	c82940_g11_i8	−1.40	**23.41**	−11.39	2.75
Fibroblast growth factor receptor 3 isoform X5	c82940_g2_i2	2.90	**8.71**	−1.05	2.85
Hyaluronan synthase 1-like	c75446_g1_i4	2.33	**18.41**	−6.94	1.16
Vascular endothelial growth factor	c74074_g2_i1	2.30	**3.06**	1.77	**2.30**

[38] and blue catfish [23]. Our present work examined the effectiveness of two prebiotic feed additives, a yeast mannan oligosaccharide (MOS) product (Actigen®) and a fungal enzyme product (Allzyme® SSF) to modulate infectivity of a virulent genomovar of *F. columnare* in channel catfish. Our results indicated a protective benefit gained through addition of Actigen® to a basal catfish diet leading us to examine gene expression patterns in the gill tissue of catfish fed both diets.

While the use of mannan oligosaccharide (MOS) products have increased in livestock feeds in recent years, the mechanisms by which they provide protection against disease are still poorly understood. Two main protective effects are hypothesized, direct blocking of pathogen colonization blocking and immune stimulation [39]. Bacterial adhesion can be mediated by interactions with carbohydrate-binding lectins [40], and this interaction can be disrupted through the presence of exogenous sugar ligands [22]. MOS can also act as a non-pathogenic microbial antigen, stimulating pathogen recognition and downstream signaling cascades which prime and prepare host immune responses for subsequent infection. A recent review by Torrecillas et al. [39] summarizes a diverse set of experiments on MOS-enhanced diets in fish species and examines the shared modes of action they reveal. In general, diets containing MOS promote gut epithelial integrity, change microbial flora composition, stimulate increased mucin secretion, and increase production of bactericidal proteins such as lysozyme. Beyond fish, similar mechanisms and effects have been observed in chickens [41] and pigs [42]. Analyses of gene expression changes induced by dietary MOS in fish have largely focused on key genes determined *ab initio* to be important for immune health in the gut based on mammalian models [43–45]. In contrast, we utilized RNA-seq to examine global gene expression in baseline and post-challenge samples taken from gill tissues of catfish fed diets with and without MOS. While not immediately intuitive, the prevalence of aquaculture pathogens using mucosal routes of entry other than the gut necessitates examination of the potential for cross-protection and cross-presentation of beneficial antigens (Ag) introduced through the diet. It would be expected that a small amount of dietary additives may be solubilized and contacting surface mucosa from uneaten, partially digested feeds breaking apart in the water [8]. However, a larger impact would be expected if common signaling and cross-presentation occurs among fish mucosal barriers. The presence of a common-mucosal immune system in fish, such that Ag encounters at one mucosal site induce protection and memory at distant mucosal sites, while still under debate, is supported by a growing body of research [5].

4.1. Baseline/pre-challenge differential expression (0 h)

Direct comparison between basal and Actigen®-fed catfish at 0 h (pre-challenge) revealed relatively few differentially expressed

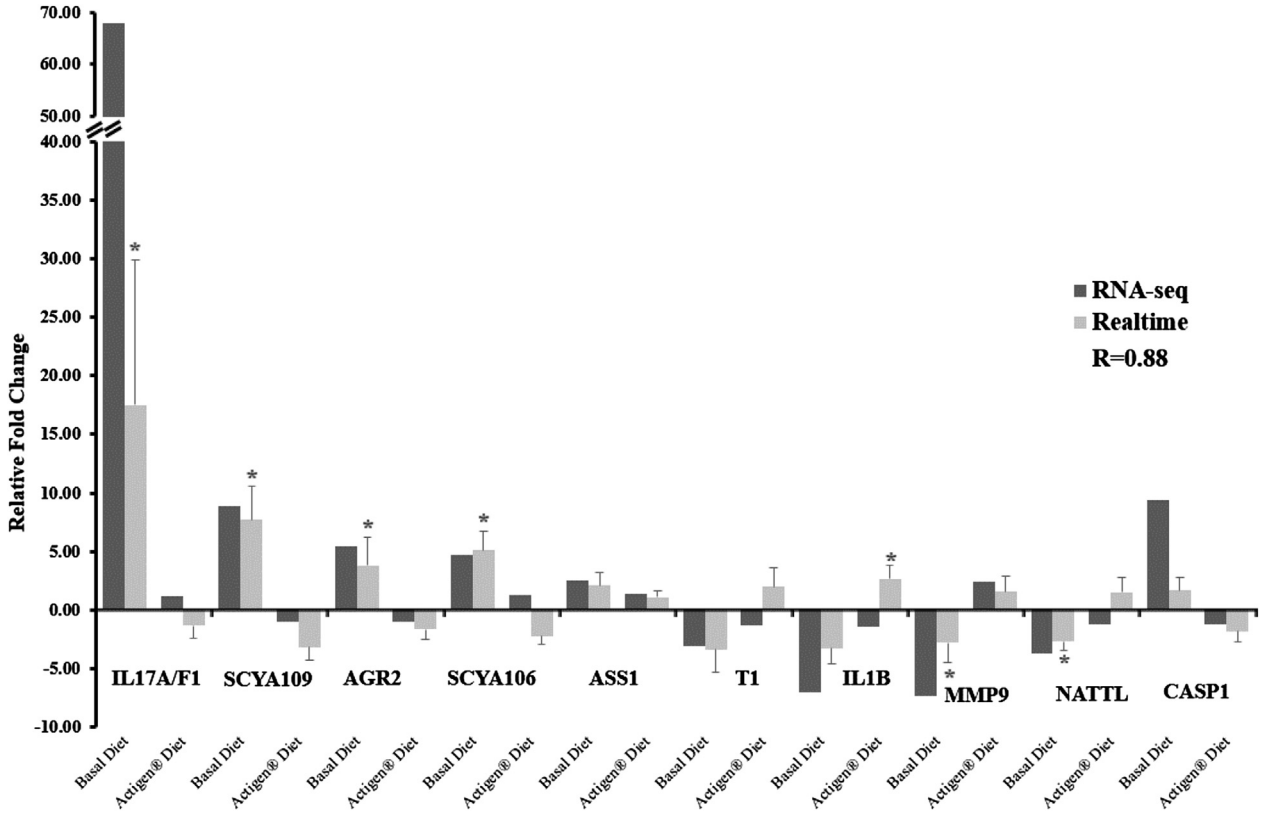

Fig. 2. Comparison of relative fold changes between RNA-seq and QPCR results in the gill from Actigen® (8 h vs 0 h) and basal diet fed catfish (8 h vs 0 h). Gene abbreviations are: Interleukin 17a/f1 precursor, IL17A/F1; CC chemokine SCYA109, SCYA109; Anterior gradient protein 2 homolog precursor, ARG2; CC chemokine SCYA106, SCYA106; Argininosuccinate synthase, ASS1; Toxin-1 precursor, T1; Interleukin-1 beta, IL1B; Matrix metalloproteinase-9 precursor, MMP9; Natterin-like protein, NATTL; Caspase-1, CASP1. Results are presented as mean ± log standard error (SE) of fold changes and the asterisk indicates statistical significance at $P < 0.05$.

genes following the eight week feeding trial (Table 8). This small number of genes was particularly striking in light of the large-scale up-regulation of genes we observed in Actigen®-fed fish soon after *F. columnare* challenge. However, among the 148 genes determined to be differentially expressed at 0 h were key signatures likely linked to a dramatic divergence in immune responses observed at 8 h. As illustrated in Fig. 4, continual antigen stimulation by MOS appears to have polarized the catfish gill mucosa toward a tolerogenic/resolution phenotype modulated in other species by Th2 and alternative (M2) macrophage cell profiles [46,47]. While baseline helper T cell and macrophage cell populations in catfish have described [48,49], further work will be needed to confirm the precise cellular actors contributing to the observed expression patterns in catfish.

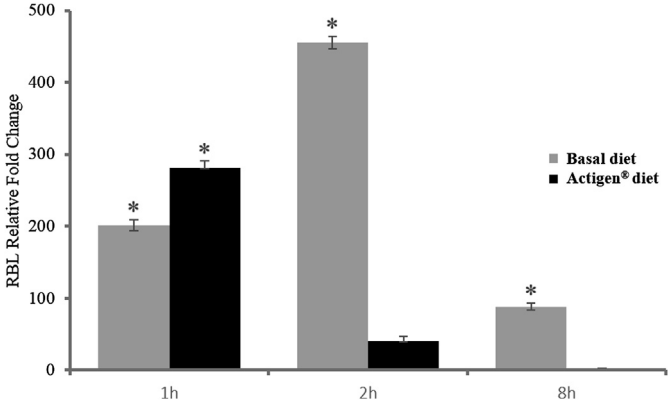

Fig. 3. QPCR analysis of RBL1a expression in the gill following *Flavobacterium columnare* infection. RBL1a expression at 1 h, 2 h, 8 h relative to control (0 h) in catfish fed Actigen® and basal diets, respectively. Results are presented as mean ± log standard error (SE) of fold changes and the asterisk indicates statistical significance at $P < 0.05$.

At the top of this proposed cascade are receptors responsible for mannose recognition, predominantly C-type lectin receptors. C-type lectin receptors (CLRs) have been found to play critical roles in determining T cell polarization fates in mammals [46]. CLRs are expressed predominantly on dendritic cells (DC) and macrophages, where, they sample antigen and present it to T cell subsets to channel the direction of subsequent immune cascades. Group I CLRs (mannose receptor family) include the mannose receptors (MR1 and MR2) and DEC205 (Ly75). Among these, mannose receptors are expressed on both macrophages and myeloid DCs, while DEC205 is expressed on myeloid DC subsets alone [50,51]. Interestingly, CLRs are valued in vaccine design strategies for their role in enhancing antigen-specific immune responses through robust antigen presentation. A series of studies have attempted to differentiate the roles of MRs and DEC205. They have revealed that: a) DEC205 is >30 times more effective in delivery of mannosylated Ags than MR; and b) DEC205 is highly upregulated on mature DC, while MR is upregulated on macrophages and dendritic cells by Th2-derived cytokines, including IL-4 [52–54]. Of great relevance here, research has shown that Ag targeting to DEC205$^+$ dendritic cells induces T cell anergy and peripheral tolerance in steady-state conditions [54–56]. With this background, a comparison of expression profiles at 0 h revealed upregulation (2.6-fold) of DEC205 in MOS-fed fish, suggesting the presence of mannose Ag-sampling dendritic cell populations in the gill lymphoid tissue.

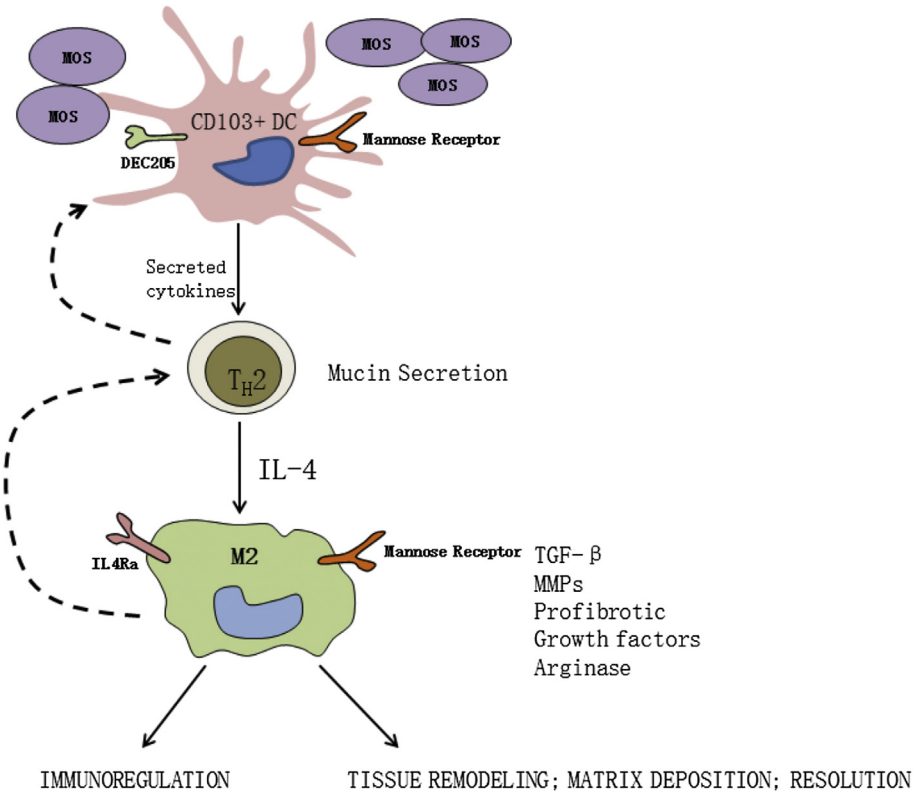

Fig. 4. Proposed MOS recognition and signaling pathways in the gill of Actigen®-fed fish, based upon RNA-seq expression signatures and known fish and mammalian signaling networks.

Supporting this assertion was the similar upregulation of CD103 (2.67-fold), a well-known marker of dendritic cell subsets, in MOS-fed fish. Indeed, pulmonary $CD103^+$ DCs prime Th2 responses to inhaled allergens [57]. Another marker of $CD103^+$ DCs, Jagged 2, was upregulated at 8 h (but not 0 h) in Actigen® (MOS) fed fish relative to the control diet (Table 8). In a study of epithelial DC populations active in Ag sampling in the lung, Sung et al. [58] again noted $CD103^+$ DCs, pointing out high levels of expression of tight junction proteins in these populations. A tight junction protein (ZO-3 like) was also upregulated here in MOS-fed fish. Notably, another receptor of immature DCs, DC-SIGN (CD209), was also differentially expressed at 0 h (down-regulated −5.59 fold). DC-SIGN, a group II CLR, interacts with a wide range of pathogens through mannose recognition and is also limited to expression on myeloid DCs [50]. Unlike DEC205, DC-SIGN can induce the differentiation of a variety of pro-inflammatory T cell classes, and has been found to be expressed on different DC subsets than DEC205 and MR [59]. Down-regulation in MOS-fed fish may reflect a shift in Ag sampling and presentation towards the more toleragenic DEC205 [60].

Among the differentially expressed genes at 0 h, additional putative evidence of MOS-driven Th2 proliferation was found. In mice, Th2 cells stimulate marked increases in mucus production, through a process dependent on IL4Rα [61]. We observed upregulation of both mucin 2 (3.46-fold) and IL4Rα (2.15-fold) at 0 h. Mucus secretion, while widely perceived as beneficial in preventing invasion of gut mucosa, can be linked with excessive inflammation and airway obstruction in the context of the mammalian lung [62]. Our previous study of catfish susceptible to *F. columnare* highlighted significantly higher mucin levels (Mucin 2, -5AC, -19) in these fish relative to resistant fish at 0 h, with declining differences at 8 h. Here Actigen®-fed fish had higher disease resistance with higher mucin expression predominantly evident at 8 h. Given the multifactorial nature of pathogenesis, further study is needed to better understand the contexts wherein mucus secretion is beneficial or detrimental in responses to *F. columnare*. Perhaps linked to increased secretion of mucus in the gill, we did observe higher levels of lysozyme in Actigen® fed fish at 0 h as we have reported previously in *F. columnare* resistant fish [4]. Lysozyme is an abundant component of mucus, linked to *F. columnare* resistance in zebrafish [63], and a common component of MOS-generated responses [41,64].

Also pointing to a role for IL-4 in the observed transcriptional responses at 0 h was the down-regulation of caspase-1. IL-4 signaling is reported to suppress caspase-1 activation, but not NLRC4, disrupting assembly of excessive inflammasomes [65]. Here we observed lower levels caspase-1 (−7.46 fold) in Actigen®-fed fish relative to the basal diet, with a NLRC5-like gene showing higher expression (2.2 fold). IL4Rα is strongly expressed on M2-alternatively-activated monocytes and macrophages and signals through Jak3 (2.11-fold higher than basal diet). Supporting the presence of M2 macrophages in higher numbers at 0 h in MOS-fed fish was the differential expression of ASS-1, involved in arginine pathways which play critical roles in the balance between M1 and M2 macrophages [66]. Furthermore, 0 h expression differences included the CC chemokine SCYA116 (3.71-fold higher), previously identified as a catfish ortholog of mammalian CCL17/CCL22 [67]. CCL17/CCL22 are well-established as chemokines important for establishing and maintaining alternatively-activated macrophage populations through signaling and positive-feedback loops between dendritic cells and macrophages [54,68,69]. Taken together, the relative handful of differentially expressed genes following the 8 week feeding trial includes important receptors involved in mannose Ag sampling, Th2 proliferation, and M2 macrophage activation which would be predicted to generate responses linked

to tolerance and tissue repair. Indeed, the 3042 differentially expressed genes following *F. columnare* challenge show the widespread transcriptional consequences of this dietary-based polarization.

4.2. Post-challenge differential expression (8 h)

The transcriptomes of Actigen®-fed and basal diet-fed catfish gill 8 h following exposure to virulent *F. columnare* were profoundly different (Tables 6 and 7), as the presence of the pathogen was met with drastically different early responses, likely due to the polarization of DC, macrophage, and T cell responses established by MOS-feeding.

Expression of components of the IL4 signaling pathway downstream of IL4Rα/JAK3 was broadly induced in Actigen®-fed fish, likely due to the increasing presence and cellular activity of M2 activated macrophages (Table 8) [70]. These included STAT6 (5.13-fold), PTPN11 (3.78-fold), IRS2 (3.44-fold) and ubiquitin ligase CBL (6.88-fold) among others [71]. While functional studies on IL-4 are lacking in catfish, recent research in other teleost fish indicates conservation of function and signaling [72,73].

M2 macrophages, upon polarization through IL-4Rα signaling, are characterized by higher mannose receptor expression, secretion of chitinases, and production of anti-inflammatory cytokines [68,69]. Expression of mannose receptors 1 and 2 (CD206 and CD280) in Actigen®-fed fish was higher relative to fish fed the basal diet (2.61-fold and 6.91-fold respectively). Expression of mannose-sampling DEC205 also continued to be higher (8.31-fold) at 8 h in Actigen®-fed fish, suggesting the continued presence of toleragenic DC cells likely reinforcing polarization. A chitinase-like protein was strongly induced (15.71-fold). In mammals, chitinase-like proteins inhibit oxidant-induced lung injury, augment Th2 immunity, regulate apoptosis, stimulate M2 macrophage activation, and contribute to wound healing [74], all processes evident in 8 h post-infection signaling in Actigen®-fed fish. TGF-β, a potent anti-inflammatory cytokine, was 3.32-fold higher in Actigen®-fed fish at 8 h. In mice, TGF-β has been found to critical for the development of airway tolerance to inhaled allergens [75].

In contrast, catfish fed the basal diet had higher expression levels of several pro-inflammatory chemokines and cytokines. The CC chemokines SCYA106, SCYA109, and SCYA113, orthologous to CCL19/21 in humans [67], were upregulated in basal fed fish. CCL19/21 signaling in mammals is important for programming of DCs for induction of Th1 responses, including release of pro-inflammatory cytokines [76]. Induction of Th17 cytokines IL-17/IL-22 was particularly pronounced in basal-diet fed fish (Table 8), rising greater than 10-fold following challenge. During lung infections, IL-17 and IL-22 drive inflammation and pathogen clearance, but can also be linked to destructive, over-exuberant responses [77]. The lack of a strong IL-17 response in the gill tissue of Actigen®-fed fish following *F. columnare* infection differs sharply from previous studies by our group and indicates the strength of the toleragenic programming induced by MOS [4,10].

Recent research has indicated that mannose receptors present on M2 macrophages are responsible for many of the immunosuppressive and tissue remodeling functions carried out by that cell type, acting as a unique bridge between innate immunity and homeostasis [50,68]. Indeed, in another potential feedback mechanism, mucins serve as MR ligands to enforce continuation of an anti-inflammatory program, particularly in toleragenic APC subsets in the gut and lung [54,78]. Higher levels of MUC17, MUC2, and MUC5AC were observed at 8 h in Actigen®-fed fish, expanding from the modestly higher mucin levels observed at 0 h (Table 8).

During proliferative and resolution phases of inflammation, M2 macrophages play a critically important role in clearance, enhancing the capacity to turnover extracellular matrix (ECM), internalizing and degrading collagen in some locations, and directing and promoting deposition in others [79]. The mannose receptors in mammals are also critical for these functions, directly recognizing, internalizing, and degrading collagen to support ECM remodeling [80,81]. Collagen degradation and turnover occurs through two pathways, an extracellular pathway in which collagen is degraded by proteases, such as matrix metalloproteinases, followed by an intracellular pathway in which M2 macrophages bind collagen through their MRs, internalize it, and degrade it using lysosomal cysteine proteinases [81,82]. It is believed that M2 macrophages may coordinate both pathways to limit peripheral damage of healthy tissue, first releasing MMPs to cleave collagen fibrils and then taking up the resulting fragments [82]. These wound healing/profibrotic macrophages additionally release TGF-β, which beyond its anti-inflammatory roles, helps to activate myofibroblasts to increase production of fibrillar collagens.

In spite of the early sampling timepoint following *F. columnare* challenge, our expression results showed abundant evidence of ECM remodeling in Actigen®-fed fish, but not in basal-diet fed fish (Table 8). Over 30 collagen isoform genes had higher expression in Actigen®-fed fish by direct comparison across diets, with within-diet comparisons showing only down-regulation of these genes in the basal diet. Similarly, MMP -9,-13,-15,-16, and −19 all had significantly higher expression in Actigen®-fed fish gill tissues, potentially indicating simultaneous degradation and deposition in different areas of the gill to aid in tissue repair. Cathepsin K, a lysosomal cysteine proteinase, was additionally upregulated in Actigen®-fed fish but not in the basal diet-fed fish. These observed expression signatures may represent provisional, temporary ECM repair efforts by M2 macrophages following initial pathogen entry. Cellular studies are needed, however, to confirm these putative pathways.

The multi-purpose nature of mannose receptors and their signaling pathways may provide a powerful connection between recognition of dietary mannose Ag, development of an immunosuppressive cellular phenotype, and the abundance of M2-polarized macrophages primed for rapid repair and resolution, in not only the gut but also surface mucosa (Fig. 4). While this polarization was associated with significantly higher survival and delayed onset of mortality in Actigen®-fed fish here, further research is needed to examine whether it tilts the scale too far in the direction of tolerance in surface mucosa. Challenge with a less virulent *F. columnare* strain or at a lower CFU dose, may have resulted in near complete protection for Actigen®-fed fish.

Acknowledgments

This work was funded by a contract from Alltech, Inc. (Trial 13-E-9091) with student funding for Honggang Zhao provided through a Chinese Scholarship Council award and from a fellowship from Shanghai Ocean University.

Appendix A. Supplementary data

Supplementary data related to this article can be found at http://dx.doi.org/10.1016/j.fsi.2015.07.005.

References

[1] FAO, Fishery and Aquaculture Statistics, FAO Fisheries and Aquaculture Department, Rome, 2012, 2014.
[2] N.L. Gutiérrez, R. Hilborn, O. Defeo, Leadership, social capital and incentives promote successful fisheries, Nature 470 (2011) 386–389.
[3] R.L. Naylor, R.J. Goldburg, J.H. Primavera, N. Kautsky, M.C. Beveridge, J. Clay, et al., Effect of aquaculture on world fish supplies, Nature 405 (2000)

1017–1024.
[4] E. Peatman, C. Li, B.C. Peterson, D.L. Straus, B.D. Farmer, B.H. Beck, Basal polarization of the mucosal compartment in *Flavobacterium columnare* susceptible and resistant channel catfish (*Ictalurus punctatus*), Mol. Immunol. 56 (2013) 317–327.
[5] I. Salinas, Y.A. Zhang, J.O. Sunyer, Mucosal immunoglobulins and B cells of teleost fish, Dev. Comp. Immunol. 35 (2011) 1346–1365.
[6] A. Abid, S.J. Davies, P. Waines, M. Emery, M. Castex, G. Gioacchini, et al., Dietary synbiotic application modulates Atlantic salmon (*Salmo salar*) intestinal microbial communities and intestinal immunity, Fish Shellfish Immunol. 35 (2013) 1948–1956.
[7] S.H. Hoseinifar, N. Soleimani, E. Ringø, Effects of dietary fructo-oligosaccharide supplementation on the growth performance, haemato-immunological parameters, gut microbiota and stress resistance of common carp (*Cyprinus carpio*) fry, Br. J. Nutr. 112 (2014) 1296–1302.
[8] C.C. Lazado, C.M. Caipang, Mucosal immunity and probiotics in fish, Fish Shellfish Immunol. 39 (2014) 78–89.
[9] A.M. Declercq, F. Haesebrouck, W. Van den Broeck, P. Bossier, A. Decostere, Columnaris disease in fish: a review with emphasis on bacterium-host interactions, Vet. Res. 44 (2013) 27.
[10] F. Sun, E. Peatman, C. Li, S. Liu, Y. Jiang, Z. Zhou, et al., Transcriptomic signatures of attachment, NF-κB suppression and IFN stimulation in the catfish gill following columnaris bacterial infection, Dev. Comp. Immunol. 38 (2012) 169–180.
[11] C.R. Arias, T.L. Welker, C.A. Shoemaker, J.W. Abernathy, P.H. Klesius, Genetic fingerprinting of *Flavobacterium columnare* isolates from cultured fish, J. Appl. Microbiol. 97 (2004) 421–428.
[12] C.A. Shoemaker, P.H. Klesius, C. Lim, M. Yildirim, Feed deprivation of channel catfish, *Ictalurus punctatus* (Rafinesque), influences organosomatic indices, chemical composition and susceptibility to *Flavobacterium columnare*, J. Fish Dis. 26 (2003) 553–561.
[13] M.B.R. Chowdhury, H. Wakabayashi, Effects of sodium, potassium, calcium and magnesiumions on *Flexibacter columnaris* infection in fish, Fish Pathol. 23 (1988) 237–241.
[14] H. Wakabayashi, Effect of environmental conditions on the infectivity of *Flexibacter columnaris* to fish, J. Fish Dis. 14 (1991) 279–290.
[15] B.D. Farmer, A.J. Mitchell, D.L. Straus, The effect of high total ammonia concentration on the survival of channel catfish experimentally infected with *Flavobacterium columnare*, J. Aquat. Anim. Health 23 (2011) 162–168.
[16] C.R. Arias, W. Cai, E. Peatman, S.A. Bullard, Catfish hybrid *Ictalurus punctatus* x *I. furcatus* exhibits higher resistance to columnaris disease than the parental species, Dis. Aquat. Organ 100 (2012) 77–81.
[17] H.S. Davis, A New Bacterial Disease of Fresh-water Fishes. Bulletin of the United States Bureau of Fisheries, GPO, Washington, 1922, pp. 261–280.
[18] B.C. Peterson, N.J. Booth, F.T. Barrows, B.B. Manning, Improved survival in channel catfish fed mannanoligosaccharides in an extruded diet, Open J. Anim. Sci. 2 (2012) 57–61.
[19] B.C. Peterson, T.C. Bramble, B.B. Manning, Effects of Bio-Mos® on growth and survival of channel catfish challenged with *Edwardsiella ictaluri*, J. World Aquacult. Soc. 41 (2010) 149–155.
[20] K. Shahzad, J.J. Loor, Application of top-down and bottom-up systems approaches in ruminant physiology and metabolism, Curr. Genomics 13 (2012) 379–394.
[21] Z. Wang, M. Gerstein, M. Snyder, RNA-Seq: a revolutionary tool for transcriptomics, Nat. Rev. Genet. 10 (2009) 57–63.
[22] B.H. Beck, B.D. Farmer, D.L. Straus, C. Li, E. Peatman, Putative roles for a rhamnose binding lectin in *Flavobacterium columnare* pathogenesis in channel catfish *Ictalurus punctatus*, Fish Shellfish Immunol. 33 (2012) 1008–1015.
[23] C. Li, B.H. Beck, E. Peatman, Nutritional impacts on gene expression in the surface mucosa of blue catfish (*Ictalurus furcatus*), Dev. Comp. Immunol. 44 (2014) 226–234.
[24] W. Thongda, C. Li, Y. Luo, B.H. Beck, E. Peatman, L-rhamnose-binding lectins (RBLs) in channel catfish, *Ictalurus punctatus*: characterization and expression profiling in mucosal tissues, Dev. Comp. Immunol. 44 (2014) 320–331.
[25] D.M. Hooge, J.L. Pierce, K.W. McBride, P.J. Rigolin, Meta-analysis of broiler chicken trials using diets with or without Allzyme® SSF enzyme complex, Int. J. Poult. Sci. 9 (2010) 819–823.
[26] O. Olivares-Fuster, S.A. Bullard, A. McElwain, M.J. Llosa, C.R. Arias, Adhesion dynamics of *Flavobacterium columnare* to channel catfish *Ictalurus punctatus* and zebrafish *Danio rerio* after immersion challenge, Dis. Aquat. Organ 96 (2011) 221–227.
[27] C. Li, R. Wang, B. Su, Y. Luo, J. Terhune, B. Beck, et al., Evasion of mucosal defenses during *Aeromonas hydrophila* infection of channel catfish (*Ictalurus punctatus*) skin, Dev. Comp. Immunol. 39 (2013) 447–455.
[28] M.G. Grabherr, B.J. Haas, M. Yassour, J.Z. Levin, D.A. Thompson, I. Amit, et al., Full-length transcriptome assembly from RNA-Seq data without a reference genome, Nat. Biotechnol. 29 (2011) 644–652.
[29] B.J. Haas, A. Papanicolaou, M. Yassour, M. Grabherr, P.D. Blood, J. Bowden, et al., *De novo* transcript sequence reconstruction from RNA-seq using the Trinity platform for reference generation and analysis, Nat. Protoc. 8 (2013) 1494–1512.
[30] K.A. Baggerly, L. Deng, J.S. Morris, C.M. Aldaz, Differential expression in SAGE: accounting for normal between-library variation, Bioinformatics 19 (2003) 1477–1483.
[31] M.D. Robinson, A. Oshlack, A scaling normalization method for differential expression analysis of RNA-seq data, Genome Biol. 11 (2010) R25.
[32] S. Bauer, S. Grossmann, M. Vingron, P.N. Robinson, Ontologizer 2.0—a multifunctional tool for GO term enrichment analysis and data exploration, Bioinformatics 24 (2008) 1650–1651.
[33] S. Grossmann, S. Bauer, P.N. Robinson, M. Vingron, Improved detection of overrepresentation of gene-ontology annotations with parent–child analysis, Bioinformatics 23 (2007) 3024–3031.
[34] M.W. Pfaffl, G.W. Horgan, L. Dempfle, Relative expression software tool (REST©) for group-wise comparison and statistical analysis of relative expression results in real-time PCR, Nucleic Acids Res. 30 (2002) e36.
[35] S.H. Chee, P.A. Iji, M. Choct, L.L. Mikkelsen, A. Kocher, Characterisation and response of intestinal microflora and mucins to manno-oligosaccharide and antibiotic supplementation in broiler chickens, Br. Poult. Sci. 51 (2010) 368–380.
[36] D. Gomez, J.O. Sunyer, I. Salinas, The mucosal immune system of fish: the evolution of tolerating commensals while fighting pathogens, Fish Shellfish Immunol. 35 (2013) 1729–1739.
[37] L. Tacchi, R. Musharrafieh, E.T. Larragoite, K. Crossey, E.B. Erhardt, S.A. Martin, et al., Nasal immunity is an ancient arm of the mucosal immune system of vertebrates, Nat. Commun. 5 (2014) 5205.
[38] L. Liu, C. Li, B. Su, B.H. Beck, E. Peatman, Short-term feed deprivation alters immune status of surface mucosa in channel catfish (*Ictalurus punctatus*), PLoS One 8 (2013) e74581.
[39] S. Torrecillas, D. Montero, M. Izquierdo, Improved health and growth of fish fed mannan oligosaccharides: potential mode of action, Fish Shellfish Immunol. 36 (2014) 525–544.
[40] C. Bavington, C. Page, Stopping bacterial adhesion: a novel approach to treating infections, Respiration 72 (2005) 335–344.
[41] R. Xiao, R.F. Power, D. Mallonee, K. Routt, L. Spangler, A.J. Pescatore, et al., Effects of yeast cell wall-derived mannan-oligosaccharides on jejunal gene expression in young broiler chickens, Poult. Sci. 91 (2012) 1660–1669.
[42] T.M. Che, R.W. Johnson, K.W. Kelley, W.G. Van Alstine, K.A. Dawson, C.A. Moran, et al., Mannan oligosaccharide modulates gene expression profile in pigs experimentally infected with porcine reproductive and respiratory syndrome virus, J. Anim. Sci. 89 (2011) 3016–3029.
[43] B. Liu, L. Xu, X. Ge, J. Xie, P. Xu, Q. Zhou, et al., Effects of mannan oligosaccharide on the physiological responses, HSP70 gene expression and disease resistance of Allogynogenetic crucian carp (*Carassius auratus gibelio*) under *Aeromonas hydrophila* infection, Fish. Shellfish Immunol. 34 (2013) 1395–1403.
[44] J. Lokesh, J.M. Fernandes, K. Korsnes, O. Bergh, M.F. Brinchmann, V. Kiron, Transcriptional regulation of cytokines in the intestine of Atlantic cod fed yeast derived mannan oligosaccharide or β-glucan and challenged with *Vibrio anguillarum*, Fish Shellfish Immunol. 33 (2012) 626–631.
[45] S. Torrecillas, D. Montero, M.J. Caballero, L. Robaina, M.J. Zamorano, J. Sweetman, et al., Effects of dietary concentrated mannan oligosaccharides supplementation on growth, gut mucosal immune system and liver lipid metabolism of European sea bass (*Dicentrarchus labrax*) juveniles, Fish Shellfish Immunol. 42 (2015) 508–516.
[46] T. Yamaguchi, F. Katakura, K. Someya, J.M. Dijkstra, T. Moritomo, T. Nakanishi, Clonal growth of carp (*Cyprinus carpio*) T cells in vitro: long-term proliferation of Th2-like cells, Fish Shellfish Immunol. 34 (2013) 433–442.
[47] S. Yoon, S. Mitra, C. Wyse, A. Alnabulsi, J. Zou, E.M. Weerdenburg, et al., First demonstration of antigen induced cytokine expression by CD4-1$^+$ lymphocytes in a Poikilotherm: studies in Zebrafish (*Danio rerio*), PLoS One 10 (2015) e0126378.
[48] N.W. Miller, R.C. Sizemore, L.W. Clem, Phylogeny of lymphocyte heterogeneity: the cellular requirements for in vitro antibody responses of channel catfish leukocytes, J. Immunol. 134 (1985) 2884–2888.
[49] S. Majji, V. Thodima, A. Arnizaut, Y. Deng, W. May, D. Sittman, et al., Expression profiles of cloned channel catfish (*Ictalurus punctatus*) lymphoid cell lines and mixed lymphocyte cultures, Dev. Comp. Immunol. 33 (2009) 224–234.
[50] T.B. Geijtenbeek, S.I. Gringhuis, Signalling through C-type lectin receptors: shaping immune responses, Nat. Rev. Immunol. 9 (2009) 465–479.
[51] J. Tel, D. Benitez-Ribas, S. Hoosemans, A. Cambi, G.J. Adema, C.G. Figdor, et al., DEC-205 mediates antigen uptake and presentation by both resting and activated human plasmacytoid dendritic cells, Eur. J. Immunol. 41 (2011) 1014–1023.
[52] S.A. Linehan, L. Martinez-Pomares, S. Gordon, Mannose receptor and scavenger receptor: two macrophage pattern recognition receptors with diverse functions in tissue homeostasis and host defense, Adv. Exp. Med. Biol. 479 (2000) 1–14.
[53] K. Mahnke, M. Guo, S. Lee, H. Sepulveda, S.L. Swain, M. Nussenzweig, et al., The dendritic cell receptor for endocytosis, DEC-205, can recycle and enhance antigen presentation via major histocompatibility complex class II-positive lysosomal compartments, J. Cell Biol. 151 (2000) 673–684.
[54] M. Chieppa, G. Bianchi, A. Doni, A. Del Prete, M. Sironi, G. Laskarin, et al., Cross-linking of the mannose receptor on monocyte-derived dendritic cells activates an anti-inflammatory immunosuppressive program, J. Immunol. 171 (2003) 4552–4560.
[55] D. Hawiger, K. Inaba, Y. Dorsett, M. Guo, K. Mahnke, M. Rivera, et al., Dendritic cells induce peripheral T cell unresponsiveness under steady state conditions in vivo, J. Exp. Med. 194 (2001) 769–779.
[56] S. Ring, M. Maas, D.M. Nettelbeck, A.H. Enk, K. Mahnke, Targeting of

autoantigens to DEC205$^+$ dendritic cells in vivo suppresses experimental allergic encephalomyelitis in mice, J. Immunol. 191 (2013) 2938–2947.
[57] H. Nakano, M.E. Free, G.S. Whitehead, S. Maruoka, R.H. Wilson, K. Nakano, et al., Pulmonary CD103(+) dendritic cells prime Th2 responses to inhaled allergens, Mucosal Immunol. 5 (2012) 53–65.
[58] S.S. Sung, S.M. Fu, C.E. Rose Jr., F. Gaskin, S.T. Ju, S.R. Beaty, A major lung CD103 (alphaE)-beta7 integrin-positive epithelial dendritic cell population expressing Langerin and tight junction proteins, J. Immunol. 176 (2006) 2161–2172.
[59] A. Engering, T.B. Geijtenbeek, S.J. van Vliet, M. Wijers, E. van Liempt, N. Demaurex, et al., The dendritic cell-specific adhesion receptor DC-SIGN internalizes antigen for presentation to T cells, J. Immunol. 168 (2002) 2118–2126.
[60] Y. Van Kooyk, W.W. Unger, C.M. Fehres, H. Kalay, J.J. García-Vallejo, Glycan-based DC-SIGN targeting vaccines to enhance antigen cross-presentation, Mol. Immunol. 55 (2013) 143–145.
[61] L. Cohn, R.J. Homer, H. MacLeod, M. Mohrs, F. Brombacher, K. Bottomly, Th2-induced airway mucus production is dependent on IL-4Ralpha, but not on eosinophils, J. Immunol. 162 (1999) 6178–6183.
[62] A. James, N. Carroll, Theoretic effects of mucus gland discharge on airway resistance in asthma, Chest 107 (1995) 110S.
[63] R. Yazawa, I. Hirono, T. Aoki, Transgenic zebrafish expressing chicken lysozyme show resistance against bacterial diseases, Transgenic Res. 15 (2006) 385–391.
[64] T.L. Welker, C. Lim, M. Yildirim-Aksoy, P.H. Klesius, Effect of short-term feeding duration of diets containing commercial whole-cell yeast or yeast subcomponents on immune function and disease resistance in channel catfish, *Ictalurus punctatus*, J. Anim. Physiol. Anim. Nutr. (Berl) 96 (2012) 159–171.
[65] I. Hwang, J. Yang, S. Hong, E. Ju Lee, S.H. Lee, T. Fernandes-Alnemri, et al., Non-transcriptional regulation of NLRP3 inflammasome signaling by IL-4, Immunol. Cell. Biol. 93 (2015) 591–599, http://dx.doi.org/10.1038/icb.2014.125.
[66] M. Rath, I. Müller, P. Kropf, E.I. Closs, M. Munder, Metabolism via arginase or nitric oxide synthase: two competing arginine pathways in macrophages, Front. Immunol. 5 (2014) 532.
[67] E. Peatman, Z. Liu, Evolution of CC chemokines in teleost fish: a case study in gene duplication and implications for immune diversity, Immunogenetics 59 (2007) 613–623.
[68] F.O. Martinez, S. Gordon, The M1 and M2 paradigm of macrophage activation: time for reassessment, F1000Prime Rep. 6 (2014) 13.
[69] R. Rajaiah, D.J. Perkins, S.K. Polumuri, A. Zhao, A.D. Keegan, S.N. Vogel, Dissociation of endotoxin tolerance and differentiation of alternatively activated macrophages, J. Immunol. 190 (2013) 4763–4772.
[70] A. Pernis, B. Witthuhn, A.D. Keegan, K. Nelms, E. Garfein, J.N. Ihle, et al., Interleukin 4 signals through two related pathways, Proc. Natl. Acad. Sci. U. S. A. 92 (1995) 7971–7975.
[71] N.M. Heller, W.M. Gwinn, R.P. Donnelly, S.L. Constant, A.D. Keegan, IL-4 engagement of the type I IL-4 receptor complex enhances mouse eosinophil migration to eotaxin-1*in vitro*, PLoS One 7 (2012) e39673.
[72] T. Wang, C.J. Secombes, The evolution of IL-4 and IL-13 and their receptor subunits, Cytokine (2015 May 21) pii: S1043–4666(15)00163-5. doi: 10.1016/j.cyto.2015.04.012. [Epub ahead of print] Review. PubMed PMID: 26005057.
[73] L.Y. Zhu, P.P. Pan, W. Fang, J.Z. Shao, L.X. Xiang, Essential role of IL-4 and IL-4Rα interaction in adaptive immunity of zebrafish: insight into the origin of Th2-like regulatory mechanism in ancient vertebrates, J. Immunol. 188 (2012) 5571–5584.
[74] C.G. Lee, C.A. Da Silva, C.S. Dela Cruz, F. Ahangari, B. Ma, M.J. Kang, et al., Role of chitin and chitinase/chitinase-like proteins in inflammation, tissue remodeling, and injury, Annu Rev. Physiol. 73 (2011) 479–501.
[75] H. Michael, Y. Li, Y. Wang, D. Xue, J. Shan, B.D. Mazer, et al., TGF-β-mediated airway tolerance to allergens induced by peptide-based immunomodulatory mucosal vaccination, Mucosal Immunol. (2015), http://dx.doi.org/10.1038/mi.2015.15 (in press).
[76] B.J. Marsland, P. Bättig, M. Bauer, C. Ruedl, U. Lässing, R.R. Beerli, et al., CCL19 and CCL21 induce a potent proinflammatory differentiation program in licensed dendritic cells, Immunity 22 (2005) 493–505.
[77] M.L. Manni, K.M. Robinson, J.F. Alcorn, A tale of two cytokines: IL-17 and IL-22 in asthma and infection, Expert Rev. Respir. Med. 8 (2014) 25–42.
[78] P. Allavena, M. Chieppa, G. Bianchi, G. Solinas, M. Fabbri, G. Laskarin, et al., Engagement of the mannose receptor by tumoral mucins activates an immune suppressive phenotype in human tumor-associated macrophages, Clin. Dev. Immunol. 2010 (2010) 547179.
[79] P.J. Wermuth, S.A. Jimenez, The significance of macrophage polarization subtypes for animal models of tissue fibrosis and human fibrotic diseases, Clin. Transl. Med. 4 (2015) 2.
[80] L. Martinez-Pomares, D. Wienke, R. Stillion, E.J. McKenzie, J.N. Arnold, J. Harris, et al., Carbohydrate-independent recognition of collagens by the macrophage mannose receptor, Eur. J. Immunol. 36 (2006) 1074–1082.
[81] D.H. Madsen, D. Leonard, A. Masedunskas, A. Moyer, H.J. Jürgensen, D.E. Peters, et al., M2-like macrophages are responsible for collagen degradation through a mannose receptor-mediated pathway, J. Cell. Biol. 202 (2013) 951–966.
[82] W. McKleroy, T.H. Lee, K. Atabai, Always cleave up your mess: targeting collagen degradation to treat tissue fibrosis, Am. J. Physiol. Lung Cell. Mol. Physiol. 304 (2013) L709–L721.